

Accelerator Development Department

Brookhaven National Laboratory
Associated Universities, Inc.
Upton, New York 11973

RHIC Technical Note No. 20

Relativistic Heavy Ion Collider

E. H. Willen

August 1986

RELATIVISTIC HEAVY ION COLLIDER

E. H. Willen
Brookhaven National Laboratory
Upton, N.Y. 11973, USA

Introduction

The Relativistic Heavy Ion Collider (RHIC) is a proposed research facility (1) at Brookhaven National Laboratory to study the collision of beams of heavy ions, up to gold in mass and at beam energies up to 100 GeV/nucleon. The physics to be explored by this collider is an overlap between the traditional disciplines of nuclear physics and high energy physics and is a continuation of the planned program of light and heavy ion physics at BNL (2). The machine is to be constructed in the now-empty tunnel built for the former CBA project. Various other facilities to support the collider are either in place or under construction at BNL. The collider itself, including the magnets, is in an advanced state of design, and a construction start is anticipated in the next several years. Figure 1 shows the layout of the RHIC project on the laboratory site.

Program of Nuclear Physics

RHIC is designed to produce extreme states of matter by colliding beams of heavy ions at high energy. In such collisions, a high "temperature" of the interacting constituents is expected, resulting in an energy density greater than 10 times that of the nuclear ground state combined with low baryon number in the central region of the collision. This combination of high energy density, greater than $1 \text{ GeV}/\text{fm}^3$, and small baryon component is the primary reason for going to such very high collision energies; under these conditions nuclear matter is expected to undergo a change of phase in which the quarks making up the individual nucleons, heretofore confined to just the volume of the nucleon, become free to move about in a much larger volume.

The resulting plasma of quarks, including also the carriers of the strong interaction force, the gluons, is of great theoretical interest. It is this state of matter that is believed to have prevailed early in the formation of the universe, before the coalescence of the plasma into nucleons. Thus, the various physical theories which describe our present material universe and how it formed, including the broken symmetries required to explain observed phenomena, e.g. non-zero pion mass, can be compared to experiment at this collider (3).

The program of colliding beam experiments at the collider will complement that of fixed target experiments being planned for the AGS and at the collider at higher energy. In fixed target experiments, a more modest energy density is achieved but in an environment of highly compressed baryon-rich nuclear matter such as exists in the interior of neutron stars, black holes, and in supernova explosions.

The kinematic space to be explored by these various facilities, including also heavy ion facilities elsewhere in the world, is shown in Fig. 2. Note that only the RHIC collider reaches far into the central region where the conditions for high energy density and small baryon component that allow a phase transition to a quark-gluon plasma are satisfied.

Machine Facilities at BNL

RHIC will be the final machine in a series of existing and planned facilities at BNL for the study of heavy ion interactions. Figure 1 shows the layout of these machines on the BNL site. Their function is described in detail elsewhere (4). Briefly, ions are produced and accelerated in an existing Van de Graaff complex and sent to the existing AGS in a recently built beam line connecting the two machines. In the AGS, the ions up to 160 are captured, accelerated and sent to

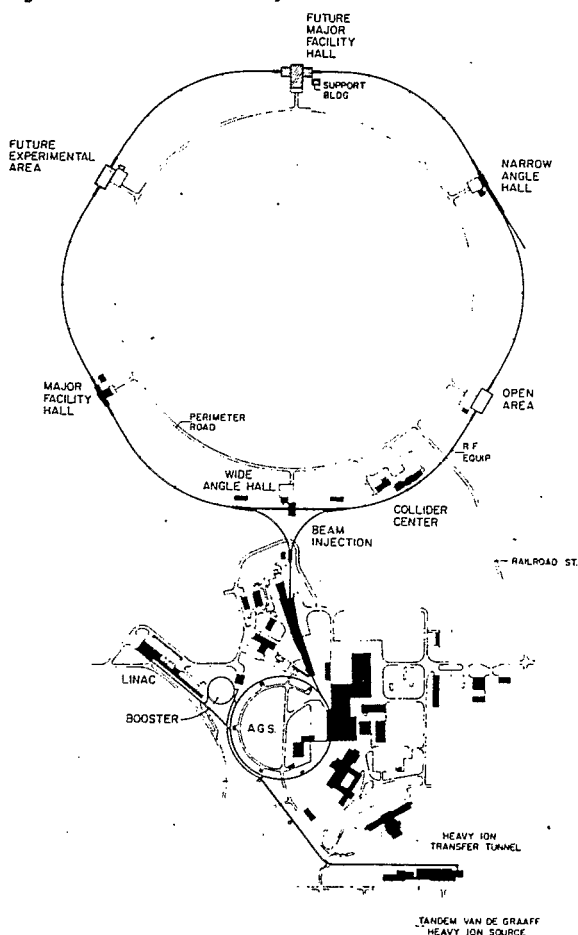


Fig. 1. Site layout of RHIC.

existing external beam lines for use by several experiments. Under construction is a booster for the acceleration of ions before injection into the AGS. This booster, by preaccelerating ions to 350

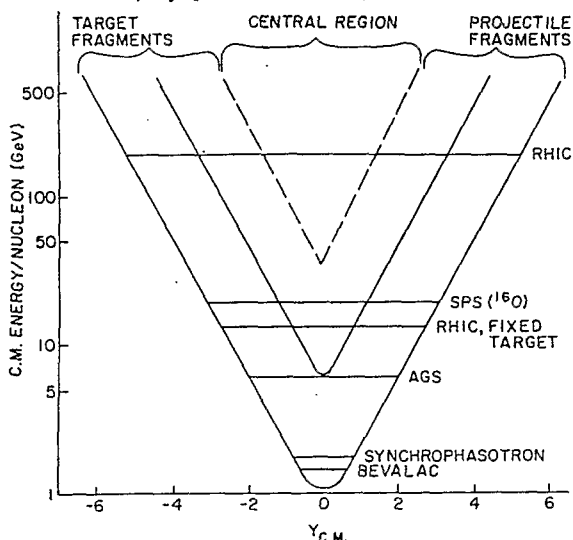


Fig. 2. The region of central collisions as a function of center-of-mass energy. The outer "V" is the kinematic boundary, the inner, solid "V" the boundary between fragmentation, or peripheral, and central collisions for protons, and the inner, dashed "V" is this same boundary for nucleus-nucleus collisions. Existing or planned facilities for heavy ion research are shown.

MeV/nucleon, will make it possible to fully strip the ions of even the heaviest species with good efficiency and thus avoid the severe losses suffered by partially-stripped ions due to residual gas scattering.

Collider Design

The machine requirements for doing physics experiments at this facility differ somewhat from those for experiments at high energy hadron-hadron colliders such as the Tevatron at FNAL and the proposed SSC. The luminosity produced by quite modest beam currents is adequate for experiments because of the high cross section for interesting events. The collider must provide colliding beams covering a wide range of energies as experiments are expected to regularly take data over the range of available energy rather than just at the highest energy. Because of the varying charge-to-mass ratio of different ions, and the interest in colliding dissimilar ion species, the collider must be capable of operation with unequal excitation in its two rings. As in any collider, long lifetime beams and stable operation are of great benefit to the experimental program.

The collider is designed to fit into the existing CBA tunnel. The tunnel circumference allows a relatively modest dipole field of 3.4 T for the required top energy of 100 GeV/nucleon for

gold beams (this corresponds to 250 GeV for protons). Beam is transferred from the AGS to fill the two rings of the collider with ion species ranging from protons to gold, including also species beyond gold with somewhat reduced performance. General parameters for the collider are given in Table 1 and some beam characteristics are given in Table 2.

Table 1. General Parameters for the Collider

Energy range (each beam),	
Au	7-100 GeV/nucleon
protons	28.5-250 GeV
Average luminosity: Au-Au,	
100 GeV/nucleon, 10 h	$4.4 \times 10^{26} \text{ cm}^{-2} \text{ sec}^{-1}$
Diamond length @ 100	
GeV/nucleon	$\pm 27 \text{ cm rms}$
Circumference (4-3/4 C _{AGS})	3833.87 m
Number of crossing points	6
Free space at crossing point	$\pm 9 \text{ m}$
Beta @ crossing,	
horizontal/vertical	6 m
low-beta insertion	3 m
Betatron tune,	
horizontal/vertical	28.82
Transition energy, Y _T	25.0
Filling mode	Box-Car
No. of bunches/ring	57
No. of Au-ions/bunch	1.1×10^9
Filling time (each ring)	$\sim 1 \text{ min}$
Magnetic rigidity, Bρ :	
@ injection	96.5 T·m
@ top energy	839.5 T·m
Beam separation in arcs	90 cm
RF frequency	26.7 MHz
RF voltage	1.2 MV
Acceleration time	1 min

Table 2. Beam Characteristics of the Collider

Element	Proton	Sulfur	Gold
Atomic number Z	1	16	79
Mass number A	1	32	197
Rest energy (GeV/nucleon)	0.9383	0.9305	0.9313
<u>Injection:</u>			
Kinetic energy (GeV/nucleon)	28.5	13.6	10.7
β	0.99947	0.99794	0.99680
Norm. emittance (π mm·mrad)	20	10	10
Bunch area (ev·sec/nucleon)	0.3	0.3	0.3
Bunch length (nsec)	± 8.6	± 8.6	± 8.6
Energy spread ($\times 10^{-4}$)	± 3.8	± 7.6	± 9.6
No. ions/bunch ($\times 10^9$)	100	6.4	1.1
<u>Top Energy:</u>			
Kinetic energy (GeV/nucleon)	250.7	124.9	100.0
Bγ	268.2	135.3	108.4

The lattice is composed of two identical, approximately circular, concentric rings in a common horizontal plane (5). Six arcs and six beam crossing points make up each ring. The polarity sequence of all quadrupoles in an arc is antisymmetric with respect to the crossing point, giving rise to a superperiodicity of three for each ring. At transition, $\gamma = 25$ so that protons are injected above transition but heavier ions must be accelerated through transition. The lattice is designed with strong focussing to reduce the aperture requirements, already large because of emittance blow-up from intrabeam scattering of the heavy ions. The lattice has 12 FODO cells per sextant, and a tune $\nu_{h,v} = 28.825$. The layout of a cell is shown in Fig. 3. Each cell is 29.622 m long, deflects the beam by 77.7 mrad and has a phase advance of 90° . The distance between the two beam centerlines is 90 cm.

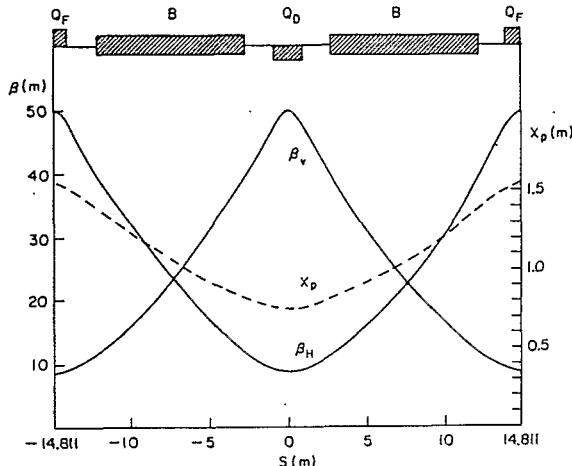


Fig. 3. RHIC regular arc cell, and the betatron (β) and dispersion (X) functions across the cell.

The crossing region lattice (insertion) is shown in Fig. 4, and the geometry of the beams near the crossing point is shown in Fig. 5. The insertions are designed to be flexible and capable of adjustment without affecting other insertions or the overall operation of the ring. The betatron function of the insertion at injection is $\beta^* = 6$; this can be adjusted to $\beta^* = 3$ at high energy for greater luminosity. The crossing angle of the beams is variable over the range 0-2 mrad. For unequal species, such as p on Au, the line of head-on collisions is rotated by 3.5 mrad with respect to the longitudinal center axis as indicated in Fig. 5. There is 10 m nominal free space on each side of a crossing, with 9 m available for experimental apparatus.

Performance

The aperture for the machine has been determined by the requirement that betatron oscillations as large as $6\sigma_\beta$, where σ_β is the rms size of the expected betatron oscillation, be contained for ten hours when $\gamma = 30$. For gold with $\gamma = 30$, the horizontal beam size corresponds to $\sigma_\beta = 1.67$ mm at $t = 0$ and grows to $\sigma_\beta = 3.0$ mm after 10

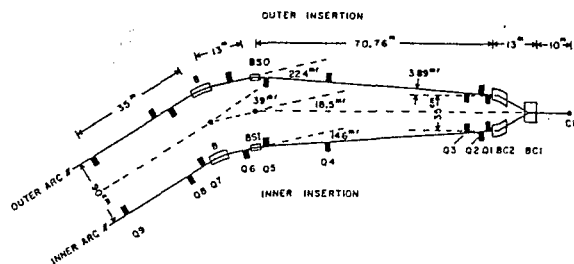


Fig. 4. Magnet layout in the crossing regions.

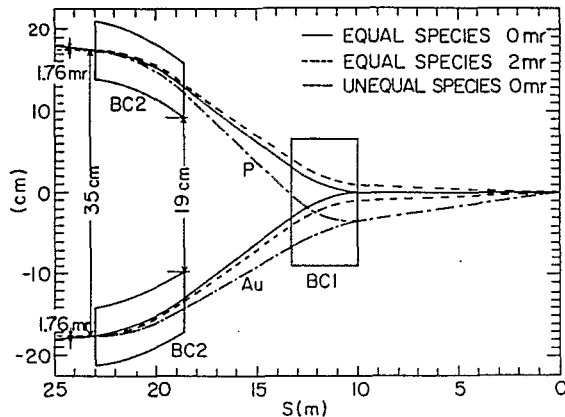


Fig. 5. Beam geometry near the crossing.

hours. Hence the required stability limit aperture, A_{SL} , is equal to 18 mm for on-momentum particles. This requirement is equivalent to an acceptance of $\sqrt{7\pi}$ mm*mrad. Using this criterion, the physical magnet aperture is determined by particle tracking studies (6), taking into account the expected field errors in the magnets. For the arc magnets, the required inner coil radius is found to be 40 mm. The growth in σ_β results from intrabeam scattering (7), a rough measure of which is given by $N_B(Z^2/A)^2$ where N_B is the number of particles per bunch, Z is the charge number and A the mass number of the ions. Intrabeam scattering imposes stringent requirements for high Z ions.

Collective effects in the collider are tolerable. The beam-beam tune shift for a given number of particles per bunch, N_B , is largest for head-on collisions of Au on Au, amounting to $\Delta\nu_v = 0.0025$ for $N_B = 1.1 \times 10^9$ at $t = 0$ but dropping to $\Delta\nu_v = 0.0009$ at $t = 10$ h as the beam dimensions increase due to intrabeam scattering. The tolerance for the longitudinal coupling impedance to limit the microwave instability within a bunch at transition is about $Z/n = 5 \Omega$. At high energy this same limit holds for protons but is considerably relaxed for heavy ions. The limit for the transverse microwave instability is more lenient by a factor of $\sqrt{5-10}$.

The physics requirements for luminosity in the collider are readily met for heavy-ion beams. The initial luminosity for head-on Au on Au at top energy is 9.2×10^{26} cm⁻²sec⁻¹, decreasing gradually with time because of beam blow up due to intrabeam scattering for an average luminosity

over 10 hours of $4.4 \times 10^{26} \text{ cm}^{-2}\text{sec}^{-1}$. In Fig. 6 is shown the average Au on Au luminosity for 2 hour and 10 hour operation as a function of the energy of the beams. Table 3 gives the initial and average luminosities at top energy for a number of different ion species.

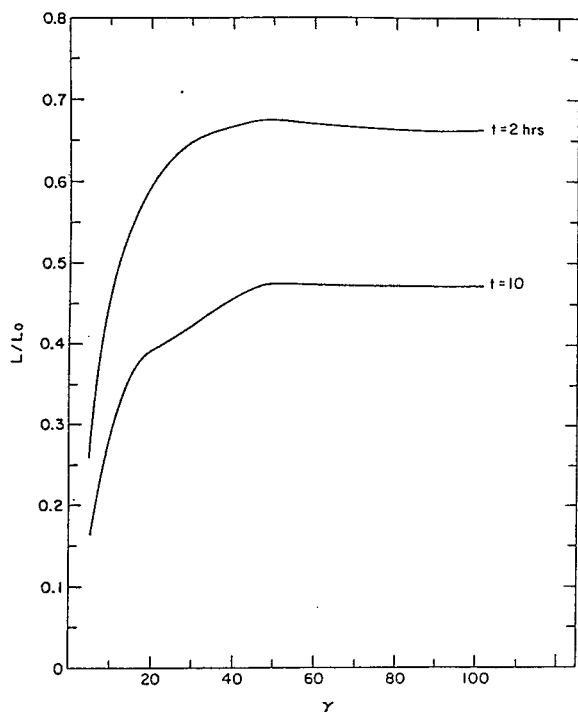


Fig. 6. Average luminosity after 2 and 10 hours divided by the luminosity at $t = 0$ as a function of energy for Au on Au, head-on collisions.

Table 3. Luminosity at Top Energy

N_B $\times 10^9$	E/A (GeV/ nucleon)	Luminosity ($\text{cm}^{-2}\text{sec}^{-1}$)				
		L_0	L_{av}	L_{av}		
		initial $\alpha=0$	10 h $\alpha=0$	10 h $\alpha=2 \text{ mrad}$		
Proton	100	250.7	9.5	8.4	4.9	$\times 10^{30}$
Deuterium	100	124.9	9.5	9.0	3.68	$\times 10^{30}$
Sulfur	6.4	124.9	3.9	2.3	0.65	$\times 10^{28}$
Gold	1.1	100	9.2	4.4	1.1	$\times 10^{26}$

Magnet System

The characteristics of the dipole and quadrupole magnets required for the arcs and for the intersection regions are given in Table 4. Table 5 lists the total complement of magnets required in the machine, including the sextupole and multipole correctors located at each of the quadrupole magnets. Current plans are for 10-20% of these magnets to be built at Brookhaven and the rest to be built in industry over a 4-year construction period.

Although there are less dipole than there are quadrupole and corrector magnets, the arc dipoles nevertheless remain the dominant cost item in the

Table 4. Characteristics of the Arc and Intersection Region Dipoles and Quadrupoles for RHIC (100 GeV/nucleon Operation)

Magnet	Coil ID (mm)	Effective Length (m)	Field or Gradient
Arc			
dipole	80	9.475	3.45 T
quadrupole	80	1.18	67.4 T/m
Intersection			
dipoles			
BC1	200	3.3	4.63 T
BC2	100	4.4	2.73 T
BS Inner	80	3.57	3.45 T
BS Outer	80	5.46	3.45 T
B	80	9.46	3.45 T
quadrupoles			
Q1-Q4	130	1.34-2.21	57.4 T/m
Q5-Q9	80	1.03-1.74	67.4 T/m

Table 5. RHIC Magnet Inventory

<u>Regular Arcs</u>	
Dipoles	288
Quadrupoles	276
Sextupoles	276
Correctors	276
<u>Intersection Regions</u>	
Standard Aperture Magnets	
Dipoles	48
Quadrupoles Q5-Q9	120
Sextupoles @ Q9	12
Correctors	144
Large Aperture Magnets	
Dipoles (BC1)	12
Dipoles (BC2)	24
Quadrupoles (Q1-Q4)	96
Correctors	72
Skew quadrupoles @ Q2 or Q3	24
<u>Totals</u>	
Dipoles	372
Quadrupoles	492
Sextupoles	288
Correctors	492
Skew quadrupoles	24

machine. For this reason, the R&D effort has focussed on this device. Various models have been built, including four in industry, culminating in a half-length model with prototype cross section that was built and tested in the past year. The successful performance of these various magnets (8) has validated the choice of design parameters, and future magnets are expected to differ only minimally from these earlier models.

A cross section of the arc dipole coil design is shown in Fig. 7. It has a single layer superconducting coil designed to provide the required 3.45 T bending field for 100 GeV/nucleon ions with a generous margin of safety. The superconductor used is the same as that used for the outer coil of the Superconducting Super Collider (SSC) magnet. Prestress is applied to the coil directly by the iron yoke through a 5 mm thick insulator-spacer surrounding the coil. The relatively close iron leads to some iron saturation field effects at high field that must be corrected with the lumped corrector magnets located at each quadrupole. There are no internal

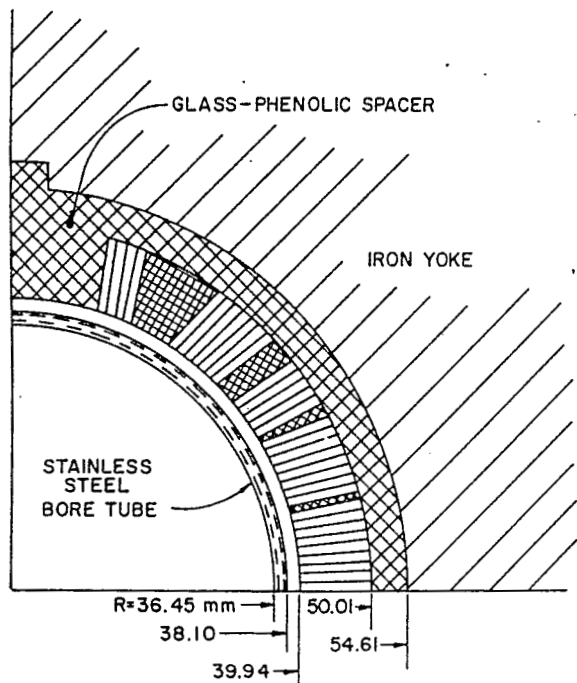


Fig. 7. Arc dipole coil cross section.

trim coils in these magnets. The 10 m long magnets are assembled in fixtures that introduce the required 47 mm sagitta during the construction process. The sagitta is locked in place via the outer stainless steel weldment, which also serves as the helium pressure vessel. The cold mass is supported in a cryostat with folded, insulating posts (originally designed by FNAL for the SSC (9)), as shown in Fig. 8. The primary design parameters for the dipole magnet and the superconductor used in its construction are given in Table 6.

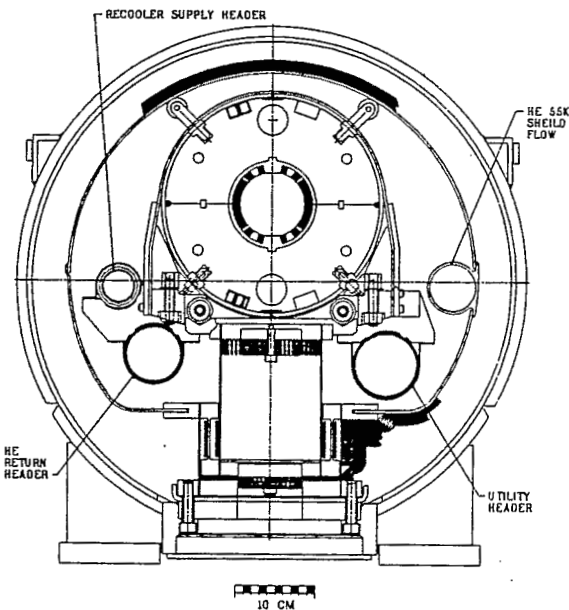


Fig. 8. Cross section of an arc dipole in cryostat.

Table 6. Basic Arc Dipole and Superconductor Parameters

Dipole Parameters	
B, minimum operation	0.24 T
B, 100 GeV/nucleon	3.45 T
B, quench	4.6 T
Current at injection	317.5 A
Current for 100 GeV/nucleon operation	4.56 kA
Inductance	43 mH
Stored energy at 100 GeV/nucleon operation	490 kJ
Length, effective	9.460 m
Sagitta	47.2 mm
Coil, number of superconducting turns	33
Coil inner radius	39.9 mm
Iron outer radius	133.3 mm
Superconductor Parameters	
Cu/SC ratio	1.8:1
Wire diameter	0.648 mm
Critical current density @ 5T, 4.2 K	2400 A/mm ²
Number of wires in cable	30
Width of cable	9.73 mm
Mid-thickness of cable	1.16 mm
Keystone angle	1.2 deg.

The design for the arc quadrupoles is shown in Fig. 9. It too is a single layer magnet using the same conductor as in the dipole and is designed to operate at the same current as the dipole. Again the use of copper wedges provides the needed degrees of freedom to achieve good field quality over the

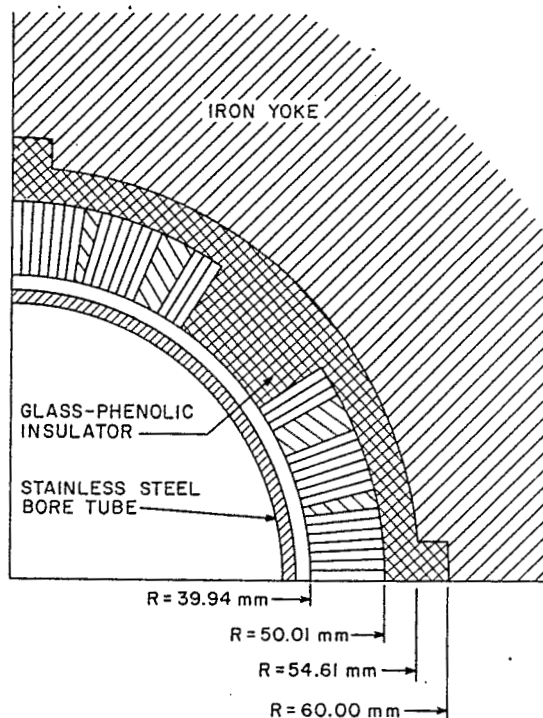


Fig. 9. Arc quadrupole coil cross section.

aperture of the magnet. The single layer design is particularly welcome in a quadrupole magnet to reduce the number of coils that must be built and assembled. The main parameters for the quadrupole are given in Table 7.

Table 7. Basic Arc Quadrupole Parameters

G, minimum operation (corresponding to 0.24T in dipole)	4.7 T/m
G, 100 GeV/nucleon	67.4 T/m
G, quench	108 T/m
Current for 100 GeV/nucleon operation	4.56 kA
Inductance	3 mH
Stored energy at 100 GeV/nucleon operation	20 kJ
Length, effective	1.24 m
Coil, number of superconducting turns	16
Coil, inner radius	39.9 mm
Iron, outer radius	133.3 mm

Summary

The design parameters of the Heavy Ion Collider have been established during the past few years and have been found to be well within the reach of available technology. The magnet system R&D has resulted in dipole models that meet the required performance specification with substantial margin. Continuing R&D in the coming year will develop quadrupole and sextupole models required in the main arcs and will lead to a string test including all components prior to full scale construction. A construction period of four years is foreseen for completion of the collider. Because of the many facilities already in place at BNL, including injector, tunnel, refrigerator and experimental halls, a cost to completion on the order of \$200 M is estimated. The unique physics potential of this facility is widely recognized (10), and its timely completion will lead to new perspectives and understandings of the fundamental properties of matter in regimes not accessible by other existing or planned facilities.

REFERENCES

1. Conceptual Design of the Relativistic Heavy Ion Collider, BNL 51932 (May 1986).
2. T. Ludlam, "Relativistic Heavy Ions at Brookhaven: High Energy Nuclear Beams in the AGS and RHIC", Proc. 2nd International Conference on Nucleus-Nucleus Collisions, Visby, Sweden (June 10-14, 1985) and BNL 37083; T. Ludlam, "Status of the RHIC Project", Proc. of the Twenty-Third Int. Conf. on High Energy Physics, Berkeley, CA (July 1986).
3. See Ref. 2 for references to more extensive discussions of the physics possibilities of relativistic nuclear collisions.
4. H. Foelsche, D.S. Barton, P. Thieberger, "Light Ion Program at BNL", Proc. 13th International Conference on High Energy Accelerators, Novosibirsk, USSR (August, 1986).
5. S.Y. Lee et al., "The RHIC Lattice", IEEE NS-32, 5, 1626 (1985) and BNL 36563. The lattice described in this paper is an earlier version of the current lattice.
6. G.F. Dell, "Particle Tracking on the BNL Relativistic Heavy Ion Collider", Proc. 13th International Conference on High Energy Accelerators, Novosibirsk, USSR (August, 1986).
7. G. Parzen, "Strong Intrabeam Scattering in Proton and Heavy Ion Beams", IEEE NS-32, 5, 2326 (1985).
8. E.H. Willen, "Magnets for RHIC", Proc. of ICFA Workshop on Superconducting Magnets, P. Dahl, Editor, BNL (May, 1986), BNL 52006. P.A. Thompson et al., "Status of Magnet System for RHIC", Proc. 2nd Conf. on the Intersections between Particle and Nuclear Physics, Lake Louise, Canada (May, 1986) and BNL 38459.
9. R.C. Niemann et al., "Design, Construction and Performance of a Post Type Cryogenic Support", Adv. Cryo. Engr. 31 (1986) Plenum Press, New York (to be published).
10. "A Long Range Plan for Nuclear Science", report of DOE/NSF Nuclear Science Advisory Committee (December, 1983).